Surface self-diffusion of hydrogen on Cu(100): A quantum kinetic equation approach

V. Pouthier and J. C. Light
The James Franck Institute, The University of Chicago, 5640 S. Ellis, Chicago, Illinois 60637

(Received 14 February 2000; accepted 17 April 2000)

The self-diffusion of hydrogen on the (100) copper surface is investigated using a quantum kinetic equation approach. The dynamics of the adatom is described with a multiple-band model and the surface phonons represent the thermal bath responsible for the diffusion mechanism. Using the Wigner distribution formalism, the diffusive motion of the adatom is characterized in terms of the correlation functions of the adatom–phonon interaction. The diffusion coefficient exhibits two terms related to phonon mediated tunneling (incoherent part) and to dephasing limited coherent motion (coherent part). The competition between these two contributions induced a transition from a thermally activated regime to an almost temperature independent regime at a crossover temperature T^*. A numerical analysis is performed using a well-established semiempirical potential to describe the adatom–surface interaction and a slab calculation to characterize the surface phonons. These calculations show that two-phonon processes represent the relevant contribution involved in the adatom–phonon coupling. The temperature dependence of the diffusion constant is thus presented and the relative contribution of the incoherent versus the coherent part is analyzed. Both contributions exhibit a change of behavior around 100 K from an exponential to a power law temperature dependence as the temperature decreases. This change is due to the confinement of the motion of the adatom in the ground energy band at low temperature. The incoherent part is shown to be the dominant contribution at high temperature and is characterized by an activation energy and a prefactor equal to $\Delta E = 0.49 \pm 0.01$ eV and $D_0 \approx 2.44 \times 10^{-3}$ cm^2/s, respectively. At low temperature, the power law dependence of the two contributions is different since the coherent part increases slowly as the temperature decreases whereas the incoherent part decreases. The crossover temperature is estimated to be equal to $T^* = 125$ K. Below T^*, the coherent part becomes the main contribution and the diffusion constant exhibits an almost temperature independent behavior. [S0021-9606(00)70227-3]

I. INTRODUCTION

Diffusion of hydrogen atoms on metallic surfaces plays a crucial role in heterogeneous catalysis and in other chemical and physical phenomena occurring at the fluid-solid interface.[1] Moreover, the diffusion of hydrogen is of fundamental interest from a basic physical point of view and gave rise to extensive theoretical and experimental studies. Due to the small mass of hydrogen, quantum effects may become important, even at room temperature, and diffusion may occur in different ways, depending on the atom–surface interaction, the coverage and the temperature. In a general way, three different mechanisms have been proposed to explain the diffusive motion of hydrogen as a function of the temperature.[2,3] In the lowest temperature regime, the diffusion may occur by tunneling from site to site. As the temperature increases, the adatom is localized in an adsorption site and diffusion consists in thermally activated uncorrelated hopping between neighboring sites. At still higher temperature, the jumps exhibit correlations and the diffusion becomes more fluidlike in character.

The principal experimental methods used to investigate surface diffusion are the field ion microscope,[3] the field emission current (FEM),[4–8] laser induced desorption,[9] scanning tunneling microscopy,[10] and laser optical diffraction (LOD).[11,12] However, for hydrogen adsorbed on metals, the experimental information is more scarce, especially in the low temperature regime where quantum effects may be important. Measurements by Gomer and co-worker using FEM have been in focus for many years.[4–8] They were the first to show the existence of a transition from a thermally activated regime to an almost temperature independent regime as the temperature decreases. Their works have suggested that band motion may play an important role at low temperature even if the bandwidth of the bands is extremely small. Note that Gomer and co-workers have shown that the system H/Ni (Ref. 8) exhibits a transition for a temperature close to 100 K. However, Zhu and co-workers[12] have performed recent experiments based on the LOD method which apparently contradict the previous results since they found a thermally activated regime as low as 65 K. Unfortunately, the authors ''do not present a satisfactory explanation for this discrepancy'' and the experimental situation remains uncertain for this system.

Two principal types of theoretical methods have been introduced to investigate the diffusion of an adatom. The first method consists in describing the motion of the adatom from a quantum mechanical point of view including the coupling with a thermal bath, either by a perturbation analysis or by

renormalization. The coupling with the substrate phonons was introduced by Kitahara *et al.*[13] to study the migration of an adatom using a one-band model. A multiple-band theory was developed by Efrima *et al.*[14,15] to investigate the role of the phonons in the thermally activated regime, i.e., disregarding the low temperature regime. The influence of both phonons and electron–hole pair excitations was discussed by Wahnstrom[16,17] using an approach based on the Fokker–Planck equation and on the friction theory. In connection with the works of Gomer, the coverage dependence of the diffusion constant was interpreted in terms of coherent band motion limited by lateral interactions.[18] The anomalous isotope dependence of the diffusion constant was studied within the small polaron formalism.[19] A two-band generalization of the Hubbard model, including the small polaron theory, was thus proposed to analyze the influence of both phonons and lateral interactions.[20]

The second type of method describes the diffusion process as a chemical reaction. These methods are based on a quantum version of the classical rate theory (TST)[21–29] or on a full quantum mechanical approach based on the flux–flux correlation function.[30] Due to the numerically demanding nature of these techniques, most of them were performed assuming a rigid surface. However, from a physical point of view, the diffusion results from a complicated interaction involving the surface dynamics. Therefore, the influence of the motion of the surface was investigated using a modified TST method[26–29] and more recently, a transition state wave packet approach.[31] The previous methods were applied to the system H/Cu(100) for which a semiempirical potential energy is available to describe the interaction between the hydrogen and the metallic surface. Note that, similar analysis were performed for other systems. For instance, the diffusion of H on Ni(100) was studied by Mattsson *et al.*[32,33] The authors have determined the potential-energy surface for this system and have analyzed the influence of the surface phonons using a path centroid method. However, even if they represent powerful techniques allowing exact quantum calculations, these second types of methods are still limited to a system which exhibits a reasonable number of degrees of freedom. In addition, they are inappropriate to describe the low temperature regime where the delocalization of the adatom may play an important role.

In this paper, the self-diffusion of hydrogen on copper is investigated using a quantum kinetic equation approach.[34,35] Such a method allows us to characterize the diffusion over a wide range of temperature, including the transition from the thermally activated regime to the low temperature regime. We describe the motion of the adatom with a multiple-band model, and the diffusion results from the dynamical coupling with the surface phonons. At low temperature, quantum effects lead to the delocalization of the adatom and to the occurrence of coherences between quantum states localized at different sites. Even if these effects are extremely weak, due to the small amplitude of the tunneling, we shall show that they are not negligible for a temperature lower than a crossover temperature. As a result, dephasing induced by surface phonons contributes significantly to the diffusion coefficient and induces a competition with the thermally activated contribution. To include these coherence effects, we generalize the multiple-band model introduced by Efrima *et al.*[14,15] using the Wigner distribution formalism.[34–37] In their works, Efrima and Metiu have neglected the influence of the coherences. Indeed, they focused on the thermally activated regime which requires one to take into account the transfers of population, only. However, the Wigner formalism is a powerful method which allows the simultaneous description of the dynamics of both coherences and populations.

The present paper is organized as follows. In Sec. II we first introduce the Hamiltonian of the whole system ''adatom+substrate'' and describe the multiple-band model in terms of the Wannier states of the adatom. Then, the Wigner function is defined and the quantum kinetic equation is established using the Zwanzig projector technique. Solving this equation, we finally introduce the self-diffusion constant of the adatom. In Sec. III we applied our formalism to the system H/Cu(100). In Sec. III A we first present the modeling of the motion of the adatom using a one-dimensional approximation. Then, the surface phonons are characterized using a slab calculation method. In Secs. III C and III D we present our results concerning the dephasing process and the temperature dependence of the diffusion constant, respectively. Finally, these results are interpreted and discussed in Sec. IV.

II. THEORETICAL PART

A. Model and Hamiltonians

We consider the quantum dynamics of a single hydrogen atom adsorbed on the (100) surface of a metallic substrate. In a general way, this dynamics is governed by the Hamiltonian of the whole system ''adatom+substrate'' which can be expressed as

$$H = H_A + H_S + V_{AS}, \tag{1}$$

where H_A denotes the Hamiltonian of the ''free'' adatom in the gas phase, i.e., the kinetic Hamiltonian, and H_S characterizes the Hamiltonian of the substrate. The third contribution, V_{AS}, stands for the potential interaction between the adatom and the surface. This coupling Hamiltonian depends on the degrees of freedom of the whole system including the position $\mathbf{x}$ of the adatom, the instantaneous positions $\{\mathbf{r}_i\}$ of the substrate atoms (surface phonons) and the electronic degrees of freedom of the surface. In this paper, we focus our attention on the influence of surface phonons and neglect the coupling between the adatom and the electronic states of the surface. Therefore, the surface dynamics correspond only to a set of small displacements $\{\mathbf{u}_i\}$ around the equilibrium positions $\{\mathbf{R}_i\}$ of the substrate atoms. As a result, we can expand the potential V_{AS} in a Taylor series with respect to these displacements, as

$$V_{AS}(\mathbf{x},\{\mathbf{r}_i\}) = V^0_{AS}(\mathbf{x},\{\mathbf{R}_i\}) + \Delta H_{AS}(\mathbf{x},\{\mathbf{u}_i\}), \tag{2}$$

where V^0_{AS} is the contribution of the potential interaction which is evaluated for the substrate equilibrium. The dependence of the potential with respect to the surface dynamics is thus contained in ΔH_{AS}. This procedure allows us to renor-

malize the Hamiltonian of the free adatom and to express the total Hamiltonian [Eq. (1)] as the sum of three contributions, as

$$H=\tilde{H}_A+H_S+\Delta H_{AS}(\mathbf{x},\{\mathbf{u}_i\}), \tag{3}$$

where $\tilde{H}_A=H_A+V_{AS}^0$. From Eq. (3), we define the system of interest as the adatom dressed by the static field created by the substrate. The purpose of this work is thus to study the quantum dynamics of this system which is naturally described by the renormalized Hamiltonian $\tilde{H}_A$. However, the adatom is not isolated and interacts with its surrounding which is defined by the surface dynamics. Consequently, the substrate acts as a thermal bath which allows the adatom to exchange energy and to relax. The dynamical coupling between the adatom and the thermal bath is described by the last contribution of Eq. (3), namely ΔH_{AS}, which is assumed to remain weak.

The first step to study the quantum dynamics of the adatom consists in characterizing its quantum states. The two-dimensional periodicity of the system allows us to seek these quantum states as Bloch states. However, the structure of these states depends strongly on the nature of the static interaction determined by the strength of the substrate corrugation. Indeed, for a sufficiently strong corrugation, the adatom is trapped in an adsorption site leading to a local behavior of its quantum states. By contrast, a weak corrugation allows the adatom to behave as a nearly free particle and a plane wave description appears to be more accurate. In this work, we are concerned with the first situation in which the strong corrugation leads to a localization of the adatom. The adsorption sites form a two-dimensional lattice of N sites located at the positions $\{\mathbf{x}_l\}$, $l=1,...,N$. Consequently, we can take advantage of this local behavior to seek the Bloch states using an empirical tight-binding method. To do so, we first solve the renormalized Hamiltonian $\tilde{H}_A$ reducing the system to a single site l and neglecting the presence of the other sites. This procedure allows us to define a set of localized orthogonal states $\{|\varphi_{ls}\rangle\}$, where $s=0,...,n$ corresponds to the state number and l to the site. Due to the tunneling mechanism, the adatom can make transitions between states which are located at different sites. As a result, the true eigenstates of $\tilde{H}_A$ can be expressed as a combination of local states centered at the adsorption sites, as

$$|\phi_{\mathbf{k}\sigma}\rangle=\frac{1}{\sqrt{N}}\sum_{ls}|\varphi_{ls}\rangle c_{s\sigma\mathbf{k}}e^{-i\mathbf{k}\mathbf{x}_l}, \tag{4}$$

where $|\phi_{\mathbf{k}\sigma}\rangle$ denotes the Bloch states with two-dimensional wave vector $\mathbf{k}$ and with a band index σ. The coefficients $c_{s\sigma\mathbf{k}}$ can easily be computed since they represent the eigenstates of the space Fourier transform of $\tilde{H}_A$ within the local basis representation. The corresponding eigenenergies are the energy bands $E_{\mathbf{k}\sigma}$.

At this step, the knowledge of the local basis allows us to describe the motion of the adatom under the influence of the renormalized Hamiltonian. We can study the quantum dynamics of the adatom either in the local basis or in the extended Bloch basis. In the following, we shall study the diffusive motion of the adatom using a quantum kinetic equation. This equation is based on a real space analysis of the motion of the adatom. Therefore, the choice of the local basis seams to be more relevant. However, the tunneling process induces a mixing of the local states leading to the band character of the true eigenstates. To take into account this mixing and to work in the real space, we follow Efrima *et al.*[14,15] and introduce a third basis which mixes the local basis and the extended Bloch basis. This new basis is formed by Wannier states which are written as

$$|\phi_{\mathbf{x}\sigma}\rangle=\frac{1}{\sqrt{N}}\sum_{\mathbf{k}}|\phi_{\mathbf{k}\sigma}\rangle e^{i\mathbf{k}\mathbf{x}_l}, \tag{5}$$

where $\mathbf{x}=\mathbf{x}_l$ is a discrete index introduced to simplify the notation. Finally, the Hamiltonian of the whole system can be expressed in the Wannier representation, as

$$H=\sum_{\sigma}\sum_{\mathbf{x}\mathbf{x}'}|\phi_{\mathbf{x}\sigma}\rangle\tilde{H}_{A\sigma}(\mathbf{x}\mathbf{x}')\langle\phi_{\mathbf{x}'\sigma}|+H_S+\sum_{\sigma\sigma'}\sum_{\mathbf{x}\mathbf{x}'}|\phi_{\mathbf{x}\sigma}\rangle \times\Delta H_{\sigma\sigma'}(\mathbf{x}\mathbf{x}')\langle\phi_{\mathbf{x}'\sigma'}|, \tag{6}$$

where $\Delta H_{\sigma\sigma'}(\mathbf{x}\mathbf{x}')=\langle\phi_{\mathbf{x}\sigma}|\Delta H_{AS}|\phi_{\mathbf{x}'\sigma'}\rangle$ is an operator which acts in the space of the states of the thermal bath, only. The diagonal elements of this Hamiltonian characterize the fluctuations of the energy of the adatom adsorbed in a site, fluctuations due to the coupling with the thermal bath. By contrast, the nondiagonal elements represent the influence of the surface dynamics on the tunneling mechanism. As we shall see, these contributions induce two different processes which perturb the dynamics of the adatom in a different way.

B. Description of diffusion processes

The characterization of diffusion processes requires the knowledge of the space and time evolution of the distribution function $g(\mathbf{x},t)$. This function represents the probability of finding the adatom at position $\mathbf{x}$ and at time t. From this distribution, we can compute, in principle, the self-diffusion constant which is related to the long time limit of the mean square displacement of the adatom. Another way to do that is to use the phenomenological Fick's law[37] which describes the self-diffusion and which is given by

$$\frac{\partial}{\partial t}g(\mathbf{x},t)=-D\boldsymbol{\nabla}^2 g(\mathbf{x},t), \tag{7}$$

where D is the self-diffusion coefficient. By Fourier transform Eq. (7), it is straightforward to show that the dispersion relation associated to the hydrodynamic modes which correspond to self-diffusion is expressed as

$$\omega_q=-iDq^2. \tag{8}$$

Therefore, the self-diffusion coefficient can be characterized from the knowledge of the behavior of the long wavelength disturbance of the distribution function.

In our model Hamiltonian, the adatom is essentially localized around an adsorption site and can realize transitions from site to site either by tunneling or by coupling with the thermal bath. Consequently, the continuous nature of the motion can be approximated by a discrete one using the Wan-

nier representation. We thus introduce the probability $g_\sigma(\mathbf{x},t)$ of finding the adatom in a band σ and in a state located around the site $\mathbf{x}$. Moreover, due to the dynamical interaction with the substrate degrees of freedom, the true eigenstates of the adatom are not well defined. As a result, we must realize a statistical average over the states of the adatom using the density matrix formalism. Finally, we define the distribution function as

$$g_\sigma(\mathbf{x},t)=\mathrm{Tr}[e^{iLt}|\phi_{\mathbf{x}\sigma}\rangle\langle\phi_{\mathbf{x}\sigma}|\rho] =B_\sigma(\mathbf{x},\mathbf{x},t), \tag{9}$$

where ρ and L denote the initial density matrix and the Liouvillian associated to the whole system, respectively, and where the variable $B_\sigma(\mathbf{x},\overline{\mathbf{x}},t)$ is written as

$$B_\sigma(\mathbf{x},\overline{\mathbf{x}},t)=\mathrm{Tr}[e^{iLt}|\phi_{\mathbf{x}\sigma}\rangle\langle\phi_{\overline{\mathbf{x}}\sigma}|\rho]. \tag{10}$$

In a general way, the variable $B_\sigma(\mathbf{x},\overline{\mathbf{x}},t)$ characterizes the coherence between the weights of two Wannier states $|\phi_{\overline{\mathbf{x}}\sigma}\rangle$ and $|\phi_{\mathbf{x}\sigma}\rangle$ when the state of the adatom is written as a linear superimposition of such a states. This measure of the coherence, which is performed at time t, depends on the dynamical evolution of the whole system and on its history from the initial time $t=0$. Note that the distribution function $g_\sigma(\mathbf{x},t)$ is related to the diagonal element $B_\sigma(\mathbf{x},\mathbf{x},t)$. However, the characterization of the diagonal elements of the B's variables is insufficient to properly describe the diffusive motion of the adatom even if non diagonal elements do not appear explicitly in the definition of the distribution function. Indeed, diagonal and non diagonal elements mix in a complicated manner under the influence of the total Hamiltonian. Consequently, we have to study simultaneously the dynamics of these two kinds of variables. One way to achieve such a procedure is to introduce the Wigner distribution[34–37] which is defined as

$$f_\sigma(\mathbf{x},\mathbf{k},t)=\sum_{\mathbf{r}} B_\sigma(\mathbf{x}+\mathbf{r}/2,\mathbf{x}-\mathbf{r}/2,t)e^{-i\mathbf{kr}}. \tag{11}$$

The Wigner distribution is the central objet of our study which allows us to describe diffusion processes. It characterizes the influence of both coherences and populations and yields the required distribution function $g_\sigma(\mathbf{x},t)$ simply by performing the sum over $\mathbf{k}$ in Eq. (11). Moreover, one of the advantages of the Wigner function is that it presents a formal resemblance to the one-particle distribution introduced in classical statistical mechanics. In the following, we thus derive a quantum kinetic equation to define the time evolution of this distribution and use the well-known theory from nonequilibrium statistical mechanics to obtain a microscopic expression of the diffusion constant.

C. Quantum kinetic equation

To build a quantum kinetic equation for the Wigner distribution, we first consider the time evolution of the B variables. Then, performing a Fourier transform as in Eq. (11), we get the required kinetic equation.

Let us assume that at the initial time $t=0$, there is no statistical correlation between the adatom and the thermal bath. As a result, the initial density matrix can be written as

$$\rho=\rho_A\rho_S, \tag{12}$$

where ρ_A and ρ_S denote the density matrix of the adatom and of the surface, respectively. The thermal bath is supposed to be in thermal equilibrium at temperature T and the density matrix ρ_S corresponds to the Boltzmann distribution. We can therefore split the total trace into partial traces and express the B variables as

$$B_\sigma(\mathbf{x},\overline{\mathbf{x}},t)=\mathrm{Tr}_A[\rho_A\mathrm{Tr}_S[\rho_S e^{iLt}]|\phi_{\mathbf{x}\sigma}\rangle\langle\phi_{\overline{\mathbf{x}}\sigma}|], \tag{13}$$

where Tr_A and Tr_S stand for a partial trace over the degrees of freedom of the adatom and of the substrate, respectively.

To solve the dynamics of the B variables, we use the projector technique introduced by Zwanzig.[38] The projector method has demonstrated its usefulness in eliminating irrelevant information from a system and extracting only the information that is desired. In our situation, the irrelevant information appears as the dynamics of the surface degrees of freedom since we are interested in the quantum dynamics of the adatom, only. From Eq. (13) the dynamics of the substrate is naturally eliminated due to the partial trace Tr_S performed over the states of the substrate. Therefore, following Zwanzig's method and performing a second order perturbation theory with respect to the coupling ΔH_{AS}, it is straightforward to show that the B variables satisfy the equation of motion

$$\frac{\partial}{\partial t}B_\sigma(\mathbf{x},\overline{\mathbf{x}},t)=i\langle e^{iLt}\langle L\rangle_S|\phi_{\mathbf{x}\sigma}\rangle\langle\phi_{\overline{\mathbf{x}}\sigma}|\rangle-\int_0^t d\tau\langle e^{iL(t-\tau)} \times\langle\Delta L_{AS}e^{iL_0t}\Delta L_{AS}\rangle_S|\phi_{\mathbf{x}\sigma}\rangle\langle\phi_{\overline{\mathbf{x}}\sigma}|\rangle, \tag{14}$$

where $\langle\cdots\rangle_S$ stands for an average over the surface degrees of freedom, i.e., $\mathrm{Tr}_S[\cdots\rho_S]$. In Eq. (14), L_0 is the Liouvillian associated to the free Hamiltonian, i.e., the Hamiltonian of the whole system when the coupling is equal to zero, and ΔL_{AS} is the Liouvillian operator which corresponds to ΔH_{AS}. The partial trace over the substrate degrees of freedom leads to a redefinition of $\tilde{H}_A$ to incorporate the averaged value of the coupling Hamiltonian. However, to keep a simple notation, we do not change the expression of the previous Hamiltonians and proceed to the following correspondence

$$\begin{aligned}&\tilde{H}_A\rightarrow\tilde{H}_A+\langle\Delta H_{AS}\rangle_S,\\ &\Delta H_{AS}\rightarrow\Delta H_{AS}-\langle\Delta H_{AS}\rangle_S.\end{aligned} \tag{15}$$

After some algebraic manipulations, the development of Eq. (14) allows us to perform a Fourier transform and to obtain the general quantum kinetic equation for the Wigner distribution, as

$$\frac{\partial}{\partial t}f_\sigma(\mathbf{x},\mathbf{k},t)+\frac{i}{\hbar}\sum_{\mathbf{x}'}\tilde{H}_{A\sigma}(0\mathbf{x}')e^{-i\mathbf{kx}'}(f_\sigma(\mathbf{x}+\mathbf{x}'/2,\mathbf{k},t)-f_\sigma(\mathbf{x}-\mathbf{x}'/2,\mathbf{k},t)) =-\sum_{\overline{\sigma}\overline{\mathbf{x}}\overline{\mathbf{k}}}\int_0^t d\tau\, J(\mathbf{x},\mathbf{k},\sigma,\overline{\mathbf{x}},\overline{\mathbf{k}},\overline{\sigma},\tau)f_{\overline{\sigma}}(\overline{\mathbf{x}},\overline{\mathbf{k}},t-\tau), \tag{16}$$

where the memory kernel $J(\mathbf{x},\mathbf{k},\sigma,\overline{\mathbf{x}},\overline{\mathbf{k}},\overline{\sigma},\tau)$ is written as

$$
\begin{aligned}
&J(\mathbf{x},\mathbf{k},\sigma,\overline{\mathbf{x}},\overline{\mathbf{k}},\overline{\sigma},\tau)\\
&\quad=\frac{1}{N}\sum_{\mathbf{r}\overline{\mathbf{r}}}\sum_{\mathbf{x}'\sigma'}\sum_{\mathbf{x}''\sigma''}e^{i(\overline{\mathbf{k}}\overline{\mathbf{r}}-\mathbf{k}\mathbf{r})}\\
&\quad\times\langle\Delta H_{\sigma\sigma'}(\overline{\mathbf{x}}+\overline{\mathbf{r}}/2,\mathbf{x}',0)\Delta H_{\sigma'\sigma}(\mathbf{x}'',\mathbf{x}+\mathbf{r}/2,\tau)\rangle_S\\
&\quad\times U^+_{A\sigma'}(\mathbf{x}',\mathbf{x}'',\tau)U_{A\sigma}(\mathbf{x}-\mathbf{r}/2,\overline{\mathbf{x}}-\overline{\mathbf{r}}/2,\tau)\,\delta_{\sigma\overline{\sigma}}\delta_{\sigma'\sigma''}\\
&\quad-\langle\Delta H_{\overline{\sigma}\sigma}(\overline{\mathbf{x}}+\overline{\mathbf{r}}/2,\mathbf{x}',0)\Delta H_{\sigma\overline{\sigma}}(\mathbf{x}-\mathbf{r}/2,\mathbf{x}'',\tau)\rangle_S\\
&\quad\times U^+_{A\sigma}(\mathbf{x}',\mathbf{x}+\mathbf{r}/2,\tau)U_{A\overline{\sigma}}(\mathbf{x}'',\overline{\mathbf{x}}-\overline{\mathbf{r}}/2,\tau)\,\delta_{\sigma'\sigma}\delta_{\sigma''\overline{\sigma}}+\text{c.c.}
\end{aligned}
\tag{17}
$$

In Eq. (17), $U^+_{A\sigma}(\mathbf{x},\mathbf{x}',\tau)$ is the matrix element of the evolution operator of the adatom, i.e., when the coupling Hamiltonian is equal to zero. It characterizes the free propagation of the adatom in a band σ, between two states located around the sites $\mathbf{x}$ and $\mathbf{x}'$. The left-hand side of Eq. (16) characterizes the coherent motion of the adatom in the band σ which involves tunneling mechanism, only. By contrast, the right-hand side of Eq. (16) represents the influence of the thermal bath on the dynamics of the adatom. This contribution is nonlocal in space and includes all the history of the coupling between the adatom and the thermal bath. Note that to obtain Eq. (16) we use the rotating wave approximation (RWA) in order to neglect the dynamical coupling between the coherences involving Wannier states associated to different bands. Such an assumption is justified by the large differences in the energy of the different bands as we shall see later for the system H/Cu.

Due to the nonlocality, Eq. (16) cannot be solved exactly and only the use of relevant approximations will allow us to reach the microscopic expression of the diffusion constant.

The memory kernel $J(\mathbf{x},\mathbf{k},\sigma,\overline{\mathbf{x}},\overline{\mathbf{k}},\overline{\sigma},\tau)$ [Eq. (17)] involves the correlation functions of the coupling Hamiltonian ΔH_{AS}. The characteristic time of this kernel is the correlation time τ_c of the heat bath and is about 10^{-10}–10^{-12} s for the substrate phonons. We thus assume that this time scale is small compare to the time evolution of the Wigner distribution. Indeed, since the Wigner distribution represents the coherence between states which lie in a given band, its characteristic time is related to the amplitude of the tunneling mechanism. It is well known that this amplitude is very weak and ranges between $V_t=10^{-20}$ and $V_t=10^{-10}$ eV when the adatom is in its ground state. As a result, the assumption $V_t\times\tau_c\ll\hbar$ is fully valid and allows us to invoke two approximations in order to simplify Eqs. (16) and (17). First, we use the Markovian limit of the kinetic equation and second, we neglect the nondiagonal element of the evolution operator $U^+_{A\sigma}(\tau)$. The last assumption means that over a time scale of about τ_c, the adatom does not have enough time to make a transition to a neighboring site. Moreover, we assume that different types of interaction between the adatom and the thermal bath are uncorrelated. Consequently, the correlation function of two different matrix elements of the coupling Hamiltonian vanishes and only the auto correlation functions are not equal to zero. Then, since we are interested by the long wavelength behavior of the distribution function, we use the continuum approximation to develop the left-hand side of Eq. (16).[39]

As a result, the quantum kinetic equation is written as

$$
\begin{aligned}
&\frac{\partial}{\partial t}f_\sigma(\mathbf{x},\mathbf{k},t)+\mathbf{v}_{\mathbf{k}\sigma}\boldsymbol{\nabla}f_\sigma(\mathbf{x},\mathbf{k},t)\\
&\quad=+\frac{1}{N}\sum_{\overline{\mathbf{k}}\overline{\mathbf{x}}\overline{\sigma}}W_{\overline{\sigma},\overline{\mathbf{x}}\to\sigma,\mathbf{x}}f_{\overline{\sigma}}(\overline{\mathbf{x}},\overline{\mathbf{k}},t)-W_{\sigma,\mathbf{x}\to\overline{\sigma},\overline{\mathbf{x}}}f_\sigma(\mathbf{x},\overline{\mathbf{k}},t)\\
&\qquad+\frac{\Gamma_\sigma}{N}\sum_{\overline{\mathbf{k}}}\,(f_\sigma(\mathbf{x},\overline{\mathbf{k}},t)-f_\sigma(\mathbf{x},\mathbf{k},t)),
\end{aligned}
\tag{18}
$$

where $\mathbf{v}_{\mathbf{k}\sigma}=\boldsymbol{\nabla}E_{\sigma\mathbf{k}}$ is the velocity of the adatom in the band σ and where

$$
\begin{aligned}
W_{\overline{\sigma},\overline{\mathbf{x}}\to\sigma,\mathbf{x}}&=\frac{2}{\hbar^2}\,\mathrm{Re}\int_0^\infty d\tau\langle\Delta H_{\overline{\sigma}\sigma}(\overline{\mathbf{x}},\mathbf{x},0)\Delta H_{\sigma\overline{\sigma}}(\mathbf{x},\overline{\mathbf{x}},\tau)\rangle_S\\
&\quad\times U^+_{A\sigma}(\tau)U_{A\overline{\sigma}}(\tau),
\end{aligned}
\tag{19}
$$

$$
\begin{aligned}
\Gamma_{\overline{\sigma}}=\sum_{\mathbf{x},\sigma}\frac{2}{\hbar^2}\,\mathrm{Re}\int_0^\infty d\tau\langle\Delta H_{\overline{\sigma}\sigma}(\overline{\mathbf{x}},\mathbf{x},0)\Delta H_{\sigma\overline{\sigma}}(\mathbf{x},\overline{\mathbf{x}},\tau)\rangle_S\\
\times U^+_{A\sigma}(\tau)U_{A\overline{\sigma}}(\tau).
\end{aligned}
$$

The left-hand side of Eq. (18) corresponds to the free force Boltzmann equation which describes the adatom as an excitation moving freely in the band σ. The right-hand side of Eq. (18), which represents the development of the memory kernel [Eq. (17)], exhibits two contributions. The first one appears as a Pauli master equation and characterizes incoherent transitions between Wannier states induced by the coupling with the thermal bath. It has been shown by Efrima *et al.*[14,15] that the rate for such a transitions, namely $W_{\overline{\sigma},\overline{\mathbf{x}}\to\sigma,\mathbf{x}}$, describes different kinds of processes and can be written as

$$
W_{\overline{\sigma},\overline{\mathbf{x}}\to\sigma,\mathbf{x}}=W^L_{\overline{\sigma}\overline{\mathbf{x}}\to\sigma,\mathbf{x}}+W^V_{\overline{\sigma}\to\sigma}\delta_{\mathbf{x},\overline{\mathbf{x}}}.
\tag{20}
$$

In Eq. (20), W^L characterizes a lateral transition which involves two different sites and W^V stands for a vertical transition which takes place between two different bands but in the same site. In each case, the rates are related themselves by the well-known detailed balance equation. Note that a lateral transition can occur either in the same band or between two different bands. The second contribution of the right-hand site of Eq. (18) describes the dephasing mechanism responsible for the destruction of the coherence of the nondiagonal elements of the B variables.

Finally, reducing our analysis to transitions between nearest neighbor sites, the quantum kinetic equation is given by

$$\frac{\partial}{\partial t} f_\sigma(\mathbf{x},\mathbf{k},t) + \mathbf{v}_{\mathbf{k}\sigma} \nabla f_\sigma(\mathbf{x},\mathbf{k},t)$$

$$= + \frac{\Gamma_\sigma}{N} \sum_k \left(f_\sigma(\mathbf{x},\bar{\mathbf{k}},t) - f_\sigma(\mathbf{x},\mathbf{k},t) \right)$$

$$+ \frac{1}{N} \sum_{\mathbf{k}\bar{\sigma}} \tilde{W}_{\bar{\sigma}\to\sigma} f_{\bar{\sigma}}(\mathbf{x},\bar{\mathbf{k}},t) - \tilde{W}_{\sigma\to\bar{\sigma}} f_\sigma(\mathbf{x},\bar{\mathbf{k}},t)$$

$$+ a^2 W^L_{\bar{\sigma}\to\sigma} \nabla^2 f_{\bar{\sigma}}(\bar{\mathbf{x}},\bar{\mathbf{k}},t), \tag{21}$$

where $W^L_{\bar{\sigma}\to\sigma} = W_{\bar{\sigma}\mathbf{x}\to\sigma\mathbf{x}\pm\mathbf{a}}$ and $\tilde{W}_{\bar{\sigma}\to\sigma} = 2W^L_{\bar{\sigma}\to\sigma} + W^V_{\bar{\sigma}\to\sigma}$ and where a denotes the lattice parameter.

D. Self-diffusion coefficient

The quantum kinetic equation is formally equivalent to the linearized Lorentz–Boltzmann equation which describes diffusion processes in classical fluid.[37] Resibois[40] has introduced a method to obtain a microscopic expression of the self-diffusion coefficient from this kinetic equation. Therefore, we use the same procedure which consists in doing the Fourier Transform of the quantum kinetic equation and in performing a perturbative theory to reach the dispersion relation of the hydrodynamic modes [Eq. (8)]. These modes correspond to slowly varying disturbances of the Wigner distribution, in space and time, around its equilibrium value. From Eq. (21), it is easy to show that this equilibrium corresponds to an homogeneous distribution in real space and in reciprocal space. The equilibrium distribution depends only on the energy of the bands and is expressed as

$$f^{\mathrm{eq}}_\sigma = \frac{1}{N} \frac{e^{-E_\sigma/kT}}{\Sigma_\sigma e^{-E_\sigma/kT}}, \tag{22}$$

where E_σ is the energy of the band σ evaluated at the center of the Brillouin zone. Note that f^{eq}_σ does not depend on the wave vector $\mathbf{k}$ since we have assumed that the tunneling amplitude is sufficiently small to neglect the dispersion of the energy bands. Therefore, we seek a solution of the kinetic equation as

$$f_\sigma(\mathbf{x},\mathbf{k},t) = f^{\mathrm{eq}}_\sigma h_\sigma(\mathbf{x},\mathbf{k},t), \tag{23}$$

where $h_\sigma(\mathbf{x},\mathbf{k},t)$ characterizes the disturbance around the equilibrium. In order to use the method described by Resibois, it is convenient to introduce an abstract linear vector space notation by considering the distribution $h_\sigma(\mathbf{x},\mathbf{k},t)$ as the component of the vector $|h(\mathbf{x},t)\rangle$ in the representation $\{|\sigma,\mathbf{k}\rangle\}$. The scalar product in this abstract vector space is defined with respect to the transformation Eq. (23), as

$$\langle h(\mathbf{x},t)|h'(\mathbf{x},t)\rangle = \sum_{\sigma\mathbf{k}} f^{\mathrm{eq}}_\sigma h^*_\sigma(\mathbf{x},\mathbf{k},t) h'_\sigma(\mathbf{x},\mathbf{k},t). \tag{24}$$

Since the quantum kinetic equation [Eq. (21)] is linear, the dispersion relation of the hydrodynamic modes can be defined considering the behavior of one Fourier component of the distribution, only. In addition, we assume that the diffusion of the adatom is ''isotropic'' on the (100) surface, i.e., the diffusion coefficient is the same along the directions of high symmetry. We thus focus our attention on the diffusion along one such direction, denoted by *x*, and seek a solution as

$$|h(\mathbf{x},t)\rangle = |h(\mathbf{q},t)\rangle e^{i(qx-\omega_q t)}, \tag{25}$$

where q is the wave vector component parallel to the *x* direction. Using Eq. (23) and substituting Eq. (25) into Eq. (21), the quantum kinetic equation can be formally expressed as

$$(\hat{R} + iq\mathbf{u}_x\hat{\mathbf{v}} + q^2\hat{W}^L)|h(\mathbf{q})\rangle = i\omega_q|h(\mathbf{q})\rangle, \tag{26}$$

where $\mathbf{u}_x$ is a unit vector parallel to the *x* direction and where $\hat{\mathbf{v}}$ and $\hat{W}^L$ are the operators associated to the band velocity of the adatom and to the rate for the lateral transitions, respectively. In Eq. (26), $\hat{R}$ stands for the relaxation operator which accounts for the dephasing mechanism and for the incoherent transitions characterized by the rate $\tilde{W}$. The explicit expression of these operators is easily defined comparing Eq. (21) and Eq. (26), as

$$\langle \mathbf{k}\sigma|\hat{R}|\bar{\mathbf{k}}\bar{\sigma}\rangle = \left(\Gamma_\sigma + \sum_{\sigma'} \tilde{W}_{\sigma\to\sigma'} \right) \delta_{\sigma\bar{\sigma}}\delta_{\mathbf{k}\bar{\mathbf{k}}} - \frac{1}{N}(\Gamma_\sigma \delta_{\sigma\bar{\sigma}} + \tilde{W}_{\sigma\to\bar{\sigma}}),$$

$$\langle \mathbf{k}\sigma|\hat{W}^L|\bar{\mathbf{k}}\bar{\sigma}\rangle = \frac{1}{N} W^L_{\sigma\to\bar{\sigma}}\delta_{\mathbf{k}\bar{\mathbf{k}}}, \tag{27}$$

$$\langle \mathbf{k}\sigma|\hat{\mathbf{v}}|\bar{\mathbf{k}}\bar{\sigma}\rangle = \mathbf{v}_{\sigma\mathbf{k}}\delta_{\sigma\bar{\sigma}}\delta_{\mathbf{k}\bar{\mathbf{k}}}.$$

Consequently, from Eq. (26), the kinetic problem is formulated in terms of an eigenvalue problem for the relaxation operator $\hat{R}$. The equilibrium distribution, which corresponds to a spatially homogeneous and time-independent distribution, is the eigenvector $|h^{(0)}\rangle = 1$ of the relaxation operator associated to the eigenvalue $\omega^{(0)} = 0$. Note that using the definition of the scalar product Eq. (24), the eigenvector $|h^{(0)}\rangle$ is normalized. For long-wavelength disturbance, the wave vector q is thus assumed to be a small parameter and the perturbed eigenvalues of the relaxation operator can be determined using a perturbative theory. Therefore, following Resibois,[37,40] we seek solutions of Eq. (26) as

$$\omega_q = \omega^{(0)} + \omega^{(1)}q + \omega^{(2)}q^2 + \cdots,$$
$$|h(\mathbf{q})\rangle = |h^{(0)}\rangle + |h^{(1)}\rangle q + |h^{(2)}\rangle q^2 + \cdots. \tag{28}$$

Substituting Eq. (28) into Eq. (26), it is straightforward to show that $\omega^{(1)}$ is equal to zero and that the first correction of the eigenfrequency is expressed as

$$\omega^{(2)} = -i\langle h^{(0)}|\hat{W}^L|h^{(0)}\rangle - i\langle h^{(0)}|\mathbf{u}_x\hat{\mathbf{v}}(\hat{R} - i\omega^{(0)})^{-1}\mathbf{u}_x\hat{\mathbf{v}}|h^{(0)}\rangle. \tag{29}$$

As a result, the microscopic expression of the diffusion coefficient is determined comparing $\omega^{(2)}$ [Eq. (29)] and the dispersion relation of the hydrodynamic modes given by Eq. (8). The resulting coefficient is expressed as

$$D=\sum_{\sigma\sigma} f_{\sigma}^{0} a^{2} W_{\sigma\to\bar{\sigma}}^{L} + \frac{1}{N_x}\sum_{\sigma\sigma}\sum_{k_x k_x} f_{\sigma}^{0} v_{k_x\sigma}\langle k_x\sigma|\hat{R}^{-1}|\bar{k_x}\bar{\sigma}\rangle v_{\bar{k_x}\bar{\sigma}}, \tag{30}$$

where N_x is the number of sites along the x direction.

The self-diffusion coefficient exhibits two contributions. The first contribution, which is proportional to the rate of lateral transitions, is the incoherent diffusion constant defined by Efrima *et al.*[14,15] It describes processes in the course of which the surface dynamics induce fluctuations of the tunneling matrix elements between two Wannier states. As a result, the adatom, initially localized in a Wannier state, is allowed to make a transition to another state by creating or annihilating surface phonons. If the transition corresponds to an ''in band process,'' i.e., if the states belong to the same band, the process is clearly identified as phonon mediated tunneling. By contrast, if the transition involves different bands, then the process corresponds to phonon induced transitions.

The second contribution occurring in Eq. (30) is the coherent part of the diffusion constant and characterizes how the dephasing limits the band motion of the adatom. Formally, if the adatom moves in a coherent manner, its eigenstate is described by a superimposition of localized Wannier states. The phases between each component of this state are related to each other when the time evolution is described by the Hamiltonian of the adatom only. However, during this time evolution, the coupling with the thermal bath induces random fluctuations of each phase which destroys the coherence of the state. As a result, the nature of the motion of the adatom evolves from a coherent one to an incoherent one. Clearly, the coherent part of the diffusion constant, is related to the competition between the tunneling mechanism, which tends to preserve the coherence, and the dephasing constant, which characterizes the damping process. Note that Eq. (30) does not exhibit an explicit dependence with respect to the tunneling matrix elements. However, the band velocity $\mathbf{v}_{\mathbf{k}\sigma}$, related to the gradient of the energy band, depends on the tunneling amplitude.

Note that the name ''coherent diffusion coefficient'' used to describe this second contribution of the diffusion constant is introduced to distinguish this contribution from the first contribution. However, dephasing limited band motion leads to the destruction of the coherence and induces, of course, an incoherent motion.

III. APPLICATION TO SELF-DIFFUSION OF HYDROGEN ON CU(100)

A. Potential interaction and quantum states of the adatom

The modeling of the system H/Cu(100) is performed using the interaction potential introduced by Wonchoba *et al.*[28] This potential consists of a sum of pairwise interactions between the H atom and each copper atom. Each interaction has the form of a Morse potential and the parameters can be found in Refs. 28 and 31. The substrate is supposed to be unreconstructed and the (100) face exhibits a square unit cell with a lattice parameter $a=2.5327$ Å.

The minimization of the potential energy leads to an equilibrium configuration where the adatom is located in a hollow site, i.e., at the center of the unit cell. The diffusion valley belongs to the $\langle 110\rangle$ direction and the height of the potential barrier between neighboring unit cells is equal to 0.51 eV. To investigate the diffusive motion of the adatom along this direction, we reduce the system to a one-dimensional one. Therefore, the renormalized Hamiltonian includes the kinetic Hamiltonian and the potential energy experienced by the hydrogen atom along the diffusion valley. Denoting by x the $\langle 110\rangle$ direction, the potential energy $V_{AS}^{0}(x)$ is thus obtained performing a minimization of the full potential with respect to the two orthogonal degrees of freedom y and z.[25]

To characterize the local basis, we reduce the potential to a single well problem and use the FBR–DVR method based on a Gauss–Hermite quadrature.[41] We thus obtain the eigenergies $\{E_s\}$ of the adsorbed atom and the corresponding localized wave functions $\{\varphi_{ls}(x)\}$. These eigenfunctions are then used to evaluate the matrix elements of the potential between states located in neighboring sites. An accurate calculation of these matrix elements requires the accurate description of the tails of the localized wave functions, i.e., the value of the wave functions in the region between two neighboring sites. However, the FBR–DVR method does not allow us to obtain such accuracy. Indeed, a localized wave function is expanded in terms of Hermite polynomials. Since the convergence of the calculations requires the use of high order polynomials, the tail of the wave function exhibits oscillations whose the shape depends on the number of DVR points. These oscillations, which are extremely small, do not influence the calculation performed to evaluate matrix elements which involve wave functions localized in the same site. By contrast, they have a dramatic influence on the calculation of matrix elements which mix wave functions located at different sites. To solve this problem, we use a semiclassical approach to build the localized wave functions from the knowledge of the eigenenergies. This method, which is known as the uniform approximation, is described in detail in Ref. 42. The idea is that the qualitative shape of a localized wave function is dictated by the disposition of its classical turning points. For the single well problem, a localized wave function describes a bound motion between two turning points. It exhibits oscillations in the classical region, i.e., between the two turning points, and dies away outside. As a result, this wave function is expressible in terms of the corresponding wave function of the harmonic oscillator. The wave function $\varphi_{ls}(x)$ of the sth state localized in the lth site is thus written as

$$\varphi_{ls}(x)=\sqrt{\frac{2s+1-\xi^{2}(x)}{K_s(x)}}\,\Psi_s(\xi(x)), \tag{31}$$

where Ψ_s is the sth wave function of the harmonic oscillator and where $K_s(x)=\sqrt{2m(E_s-V_{AS}^{0}(x)}/\hbar$. The function $\xi(x)$ is defined by the transcendental equation

TABLE I. Energies of the seven localized bound states and tunneling amplitude between similar states lying in neighboring sites.

Level	E (eV)	V_t (eV)
0	0.0538	5.042(−14)
1	0.1547	−1.340(−11)
2	0.2432	1.374(−09)
3	0.3206	−7.316(−08)
4	0.3874	2.237(−06)
5	0.4439	−4.115(−05)
6	0.4896	4.796(−04)

$$\int_{-\xi_0}^{\xi} (\xi_0^2 - \xi^2) d\xi = \int_t^x K_s(x) dx, \tag{32}$$

where $\xi_0 = \sqrt{2s+1}$ and where t denotes the classical turning point located at the left-hand side of the minimum of the potential well.

As shown in Table I, the local basis contains seven bound states with an energy lower than the potential barrier. The ground state corresponds to an energy equal to 0.053 eV and the harmonic frequency is about 100.9 meV. The second column of Table I contains the tunneling matrix elements between localized states in neighboring unit cells which have the same energy. The extremely small amplitude of the tunneling leads to a dispersion of the five lowest energy bands less than 0.01 meV. These results show that the use of the Markovian limit to reach the final expression of the kinetic equation is a good approximation. However, the dispersion of the most excited band, equal to 1.92 meV, leads to a propagation time of the adatom about $\tau_p \approx 0.1$ ps. We thus expect that the most excited band will contribute to the diffusion at high temperature, only. Since the correlation time of the phonons bath decreases with the temperature, we assume that the Markovian limit remains valid.

B. Surface dynamics

To characterizes the surface phonons, we use an empirical force constant model implying adjustable parameters in order to fit the previous experimental and theoretical data. It has been shown that the surface relaxation of the Cu(100) substrate remains small and represents a correction which ranges between 1% and 3% with respect to the bulk structure.[43] As a result, the (100) copper surface has essentially a bulk like geometry. However, for such an open face, it has been mentioned[44] that substantial charge redistribution in the surface region can change the surface force constant value even for a surface with a geometry like the bulk.

The phonon dynamics are thus solved using a 50-layer slab calculation.[45] We restrict the interaction to nearest neighbors and introduce the nearest neighbor bulk force constant $\phi_B'' = 1.605\,\mathrm{eV\,\AA^{-2}}$. This value is in good agreement with previous calculations performed to solve the (110) surface.[46] The surface force constants have been chosen empirically to reproduce the surface dynamics. Note that, a free correction model, i.e., neglecting the change in the surface force constants, leads to results in good agreement with more sophisticated calculations[44] since the error for the frequencies of the surface phonons is less than 1.5 meV.

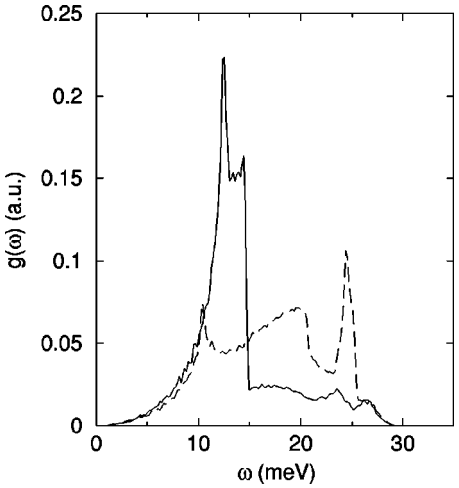

FIG. 1. Projection of the normalized density of states of the substrate phonons on the (100) copper surface. The full line characterizes the density of states associated to phonons polarized along the direction normal to the surface. The dashed line is related to phonons polarized along the direction parallel to the surface.

We show on Fig. 1 the projection of the density of states of the substrate phonons on the (100) copper surface. The full line characterizes the density of states associated to phonons polarized along the direction normal to the surface whereas the dashed line is related to phonons polarized along the direction parallel to the surface. The phonon spectrum ranges between 0 and 29.2 meV. The parallel density of states exhibits two peaks corresponding to surface modes and which are located at 10.3 meV and 24.4 meV, respectively. The frequencies of the surface modes polarized along the normal to the surface are centered around 13 meV, i.e., at 12.4 meV and 14.4 meV, respectively. Note that in the low frequency region, the density of states behaves as ω^2 as predicted by the well-known Debye model for a three-dimensional solid.[39]

From these calculations, we are able to characterize the interaction between the adatom and the substrate phonons. We thus analyze one-phonon and two-phonon processes performing a second order expansion of the interaction potential V_{AS} [Eq. (2)] with respect to the displacements of the substrate atoms. The coupling Hamiltonian between the adatom and the surface phonons can thus be defined and allows us to evaluate the correlation functions required to calculate the rates and the dephasing constant [Eq. (19)]. These correlation functions are expressed in terms of the correlation functions of the displacements of the substrate atoms and are computed from the knowledge of the phonon density of states.[45]

C. Energy corrections and dephasing constants

As mentioned in the theoretical part, the averaged value of the coupling Hamiltonian ΔH_{AS} over the thermal bath degrees of freedom leads to a correction of the renormalized Hamiltonian of the adatom [Eq. (15)]. We show in Fig. 2 the temperature dependence of the energy corrections of the seven bound states. Note that only two-phonon processes induce a nonvanishing correction to the energy levels. In a

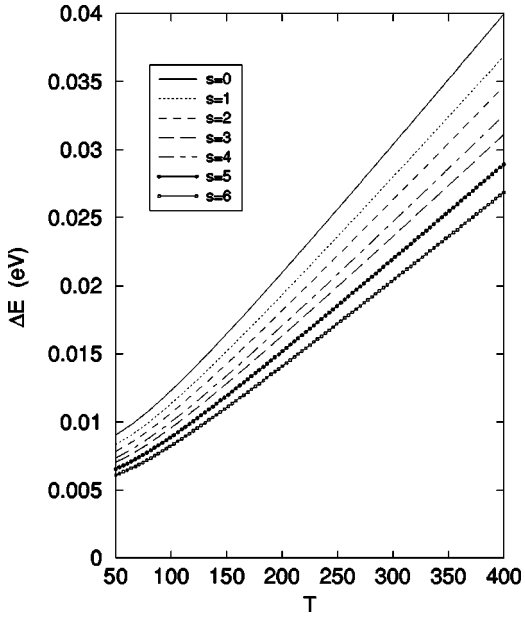

FIG. 2. Temperature dependence of the averaged value of the coupling between the adatom and the surface phonons. Only the correction of the bound states energies is shown.

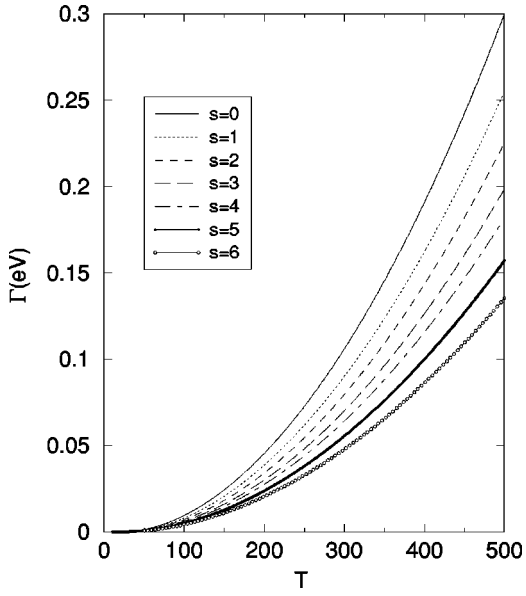

FIG. 3. Temperature dependence of the dephasing constant of each bound state.

general way, the energy correction increases with the temperature and decreases as the state number increases. The different states do not experience the same correction and this difference evolves with the temperature. Indeed, the shift of the ground state is equal to 12.30 meV at $T=100\,\mathrm{K}$ and increases up to 30.38 meV at $T=300\,\mathrm{K}$. By contrast, the correction to the most excited bound state increases from 8.26 meV to 20.32 meV in the same range of temperature leading to a dispersion of the energy shift which varies from 4.04 meV to 10.06 meV. Two-phonon processes induce a small correction of the tunneling matrix elements. At low temperature, i.e., $T=10\,\mathrm{K}$, this correction leads to a shift of the tunneling amplitude which is equal to 1.36% in the ground state and to 1.12% in the most excited state. As the temperature increases, the correction becomes more important but remains weak since it is lower than 15% at $T=1000\,\mathrm{K}$.

The behavior of the dephasing constant [Eq. (19)] with respect to the temperature is shown on Fig. 3 for the different bound states. As for the correction of the energy, the dephasing constant decreases as the energy of the bound state increases. At $T=100\,\mathrm{K}$, the dephasing constant of the ground state is equal to 9.5 meV whereas the constant characterizing the more excited state is equal to 4.3 meV. The dispersion of the value versus the energy of the bands is thus equal to 5.2 meV. This dispersion increases with the temperature and reaches, for example, a value equal to 58.1 meV at $T=300\,\mathrm{K}$. For this temperature, the dephasing constant of the ground state is equal to 0.10 eV. At low temperature, the dephasing constant shows a power law dependence of the form $\Gamma\propto T^{\alpha}$. Fitting the curve of the ground state leads to a value for the parameter α equal to $\alpha\approx 3.20\pm 0.05$. Since the different constants exhibit a similar temperature dependence, they are characterized by the same power law. Note that only two-phonon processes contribute significantly to the dephasing mechanism. For example, at $T=300\,\mathrm{K}$, the contribution of one-phonon processes represents about $2\times 10^{-3}\%$ of the dephasing constant of the ground state.

D. Incoherent, coherent, and full self-diffusion coefficient

In this section, we first present the results concerning the behavior of the incoherent rates. However, since the incoherent part of the diffusion coefficient [Eq. (30)] is directly related to the rates of interest [Eqs. (19) and (20)], we focus our attention on the values of this latter parameter. Then, from the knowledge of the dephasing constant and of the rates for the incoherent hops, we characterize the coherent contribution of the diffusion coefficient. Finally, the full coefficient is presented.

In Fig. 4 we show the temperature dependence of the incoherent diffusion coefficient D_i for one-phonon and for two-phonon processes, respectively. Clearly, as for the dephasing mechanism, two-phonon processes represent the dominant contribution of the incoherent rates, the one-phonon contribution corresponding to a correction less than 0.05%. The diffusion coefficient D_i shows an activated temperature dependence at high temperature, i.e., typically for T greater than 100 K. This behavior allows us to fit the curve with an Arrhenuis law of the form $D_i=D_0e^{-\Delta E/kT}$. The activation energy is thus equal to $\Delta E=0.49\pm 0.01\,\mathrm{eV}$ and the prefactor is given by $D_0\approx 2.44\times 10^{-3}\,\mathrm{cm^2/s}$. As shown in Table II, the incoherent diffusion constant is equal to $D_i=1.29\times 10^{-11}\,\mathrm{cm^2/s}$ at $T=300\,\mathrm{K}$ and reaches the value $D_i=1.20\times 10^{-5}\,\mathrm{cm^2/s}$ at $T=1000\,\mathrm{K}$. Note that the rates associated to one-phonon and two-phonon processes behave similarly versus the temperature since both follow an Arrhenius-type law.

At low temperature, typically for T lower than 100 K, the behavior of D_i exhibits a change and varies more slowly with the temperature. Clearly, the curve does not follow an

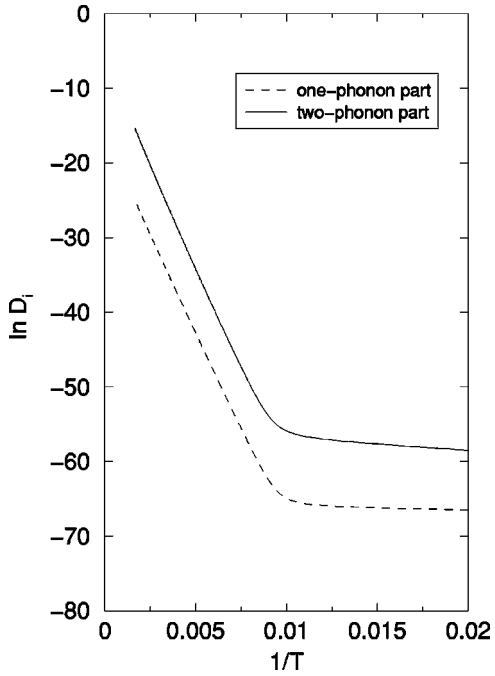

FIG. 4. Temperature dependence of the incoherent part of the diffusion coefficient. The full line corresponds to two-phonon contribution whereas the dashed line is related to one-phonon contribution.

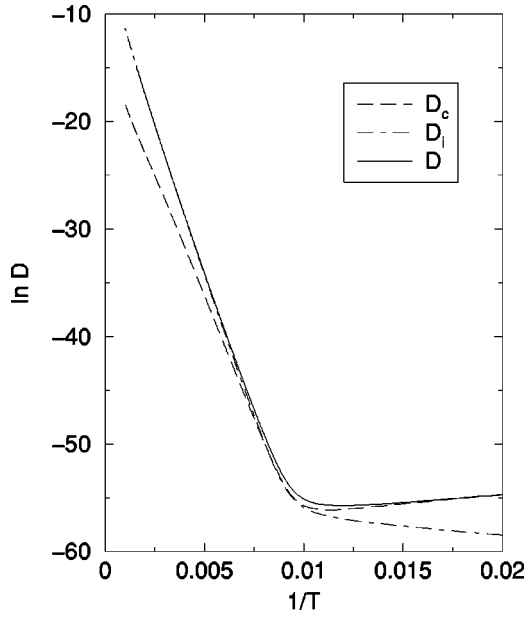

FIG. 5. Temperature dependence of both the incoherent and the coherent part of the diffusion coefficient. The full line corresponds to the full diffusion coefficient whereas the dotted line and the dashed line are related to the incoherent and to the coherent contribution, respectively.

Arrhenius-type law in this range of temperature. Moreover, one-phonon and two-phonon processes do not exhibit the same temperature dependence. Therefore, a fit of the two curves for T lower than 50 K shows a linear temperature dependence for the one-phonon contribution and a power law dependence for the two-phonon contribution. In this latter case, the parameter α characterizing the power law was found to be equal to $\alpha \approx 3.26 \pm 0.05$. Note that the temperature at which the shape of D_i exhibits a change of behavior does not correspond to a particular value. We just identify $T \approx 100\,\mathrm{K}$ as the temperature around which the change occurs.

The variation of the coherent contribution of the diffusion coefficient D_c versus the temperature is shown on Fig. 5. At high temperature, typically for T greater than 100 K, D_c increases with the temperature. However, D_c does not show an Arrhenius-type law and exhibits a slower temperature dependence compared to D_i. As shown in Table II, D_c is smaller than D_i by three orders of magnitude at $T = 1000\,\mathrm{K}$. This difference decreases as the temperature decreases and two orders of magnitude separate the two contributions at $T = 300\,\mathrm{K}$. The main difference between D_c and D_i occurs at low temperature. Indeed, for a temperature lower than 100 K, D_c exhibits a completely different behavior. First, D_c reaches a minimum value equal to $4.30 \times 10^{-25}\,\mathrm{cm^2/s}$ for $T = 88.50\,\mathrm{K}$. Then, D_c shows a change in its behavior and increases as the temperature decreases. Consequently, D_c becomes greater than D_i in this temperature range. The low temperature behavior of the coherent contribution D_c is clearly related to the variation of the dephasing constant. Indeed, when the temperature is lower than 50 K, the curve D_c versus the temperature can be fitted by a power law. The parameter α was found to be $\alpha \approx -3.22 \pm 0.05$. This value is close to the absolute value of the exponent which characterizes the low temperature behavior of the dephasing constant, i.e., $\alpha \approx 3.20 \pm 0.05$ (see Sec. III C), implying the relation $D_c \propto 1/\Gamma$.

TABLE II. Temperature dependence of the incoherent and coherent contributions of the diffusion coefficient.

T (K)	D_i ($\mathrm{cm^2/s}$)	D_c ($\mathrm{cm^2/s}$)
60	6.84(−26)	9.93(−25)
80	1.55(−25)	4.71(−25)
100	5.29(−25)	6.25(−25)
120	5.28(−23)	5.54(−23)
140	1.68(−20)	1.03(−20)
160	1.72(−18)	6.13(−19)
180	6.82(−17)	1.49(−17)
200	1.35(−15)	1.90(−16)
220	1.59(−14)	1.51(−15)
240	1.26(−13)	8.44(−15)
260	7.41(−13)	3.58(−14)
280	3.14(−12)	1.22(−13)
300	1.29(−11)	3.52(−13)
400	1.47(−09)	1.33(−11)
500	2.72(−08)	1.13(−10)
1000	1.20(−05)	1.07(−08)

The full self-diffusion coefficient D is the sum of both the coherent and incoherent mechanisms of diffusion [Eq. (30)]. As a result, the relative contribution of these two terms will depend on the temperature of interest (Fig. 5). Therefore, at high temperature, D is dominated by the incoherent contribution and is related to a thermally activated processes. The temperature dependence of D is thus described by an Arrhenius law with the same parameters as those introduced to characterize the variations of D_i. However, as the temperature decreases, the relative influence of the coherent part D_c increases. When T is close to 100 K, the two contribu-

tions D_c and D_i are nearly the same. Consequently, both coherent and incoherent mechanisms contribute to the diffusion constant and D moves away from the incoherent curve (Fig. 5). As the temperature decreases, the coherent contribution dominates the diffusion process and the coefficient D reaches the coherent curve. From these results, it seems interesting to introduce a characteristic temperature which allows us to separate the incoherent and the coherent regimes for the diffusion coefficient. We thus define this crossover temperature T^* as the temperature which corresponds to the same value for D_c and D_i, i.e., $D_c(T^*)=D_i(T^*)$. As shown on Fig. 5, the crossover temperature is thus equal to $T^*=125\,\mathrm{K}$.

IV. DISCUSSION

The previous results clearly show that the diffusion mechanism results from a dynamical interaction between the adatom and the surface whose main contribution involves two-phonon processes. Furthermore, the temperature dependence of both the incoherent and the coherent part of the diffusion coefficient changes around 100 K.

The relative contribution of one-phonon versus two-phonon processes is directly connected to the first derivative and to the second derivative of the adatom-surface potential, respectively. Consequently, the weight of each contribution depends on the matrix elements of these derivatives used to express the dephasing constant and the incoherent rates. The dephasing constant associated with a particular state is defined in terms of the correlation functions of the coupling Hamiltonian involving transitions between this state and all the other states [Eq. (19)]. However, the coupling between states located in different sites are extremely weak and the main contribution is thus due to matrix elements which connect states lying in the same site. As a result, two kinds of processes can take place in terms of phonon induced fluctuations of a given state and phonon induced transitions. Since the phonon spectrum ranges between 0 and 30 meV, resonant transitions occur between the most excited states only and take place at high temperature when the population of these states becomes significant. Therefore, the main contribution of dephasing is due to the fluctuations of the diagonal matrix elements of the coupling. When the adatom is located close to its equilibrium position, only the matrix elements of the second derivative of the potential are important leading to the negligible effect of the one-phonon processes. By contrast, the incoherent diffusion coefficient is related to the correlation functions of the nondiagonal elements of the coupling which involve states located in neighboring sites. Therefore, both one-phonon and two-phonon processes are involved in the incoherent transitions. The fact that two-phonon processes represent the main contribution results from the competition between the matrix elements of the first and second derivative of the potential, respectively.

For both the coherent and incoherent diffusion constant, the occurrence of a change in the temperature dependence is due to the competition between processes occurring in the ground state and those which take place in the excited states. At low temperature, only the ground band is significantly filled and the motion of the adatom can be viewed as a one-band motion. The coherent contribution of the diffusion coefficient, D_c, is proportional to the ratio of the square of the velocity of the adatom in this band to the dephasing constant. As shown on Fig. 5, as the temperature increases the dephasing constant increases leading to the diminution of D_c. However, when the temperature reaches 100 K, the population of the first excited band is sufficient so that coherent diffusion takes place in this band. Since the tunneling amplitude, and thus the velocity, increases with the energy of the band, the coherent diffusion in the first excited band is more important compared to diffusion in the ground state band. As a result, the increase of D_c with the temperature characterizes the transition between the motion in the ground band and the motion in the first excited band. The temperature for which such a mechanism occurs is related to the competition between the Boltzmann factor and the tunneling in the first excited state. The analysis of the numerical data shows that the temperature of interest is equal to 102 K. The same explanation can be used to interpret the behavior of the incoherent part of the diffusion constant D_i around 100 K. Indeed, the temperature dependence of D_i shows that the incoherent coefficient related to the first excited band is equal to the incoherent coefficient of the ground band at a temperature equal to 104 K.

At high temperature, the diffusion results from a thermally activated process in terms of phonon induced incoherent hops. The activation energy is different from the classical activation barrier, i.e., the potential barrier between neighboring sites equal to 0.51 eV, and corresponds to the energy of the most excited state. Note that we did not include the states lying above the corrugation. At very high temperature, these states may participate in the motion of the adatom. Nevertheless, our results are in good agreement with previous calculations performed using quantum version of the rate theory. At $T=300\,\mathrm{K}$, the diffusion constant for a rigid substrate was found to range between $1.31\times10^{-10}\,\mathrm{cm^2/s}$ and $5.01\times10^{-10}\,\mathrm{cm^2/s}$.[21–30] Landerdale *et al.*[24] have reported a value equal to $6.97\times10^{-11}\,\mathrm{cm^2/s}$ using a classical harmonic oscillator model. The correction induced by the motion of the surface was found to be extremely small[26–29] and corresponds to a factor lesser than 5 at $T=300\,\mathrm{K}$. The wave packet analysis performed by Zhang *et al.*[31] show a diffusion constant equal to $8.64\times10^{-10}\,\mathrm{cm^2/s}$ at the same temperature. As shown in Table II, our calculations yield a diffusion coefficient equal to $1.32\times10^{-11}\,\mathrm{cm^2/s}$ at $T=300\,\mathrm{K}$ leading to a difference of less than one order of magnitude with respect to these previous calculations. However, these previous results were found using techniques which are fully different from the method we used and a direct comparison must be done carefully.

The main advantage of our technique is the ability to describe the motion of the adatom at low temperature where both the coherent and incoherent mechanisms contribute significantly to the diffusion. Our results show that a transition occurs from a thermally activated regime to an almost temperature ''independent'' regime at the crossover temperature $T^*=125\,\mathrm{K}$. Below this crossover temperature, the diffusion constant follows the coherent contribution and increases as the temperature goes to zero. This feature is easily under-

standable since phonon induced dephasing depends on the population of surface phonons. Consequently, as the temperature decreases, the population of phonons diminishes and the perturbation induced by the thermal bath disappears leading to a divergence of the diffusion coefficient at zero temperature which was found to scale as $T^{-\alpha}$ with $\alpha \approx 3.2$. For surface diffusion, there is no experimental data which reports this feature. However, the behavior of the diffusion coefficient at low temperature was extensively studied for hydrogen, muon and muonium diffusion in solid.[47] In insulators, where the thermal bath is essentially composed of phonons, it as been shown, from a theoretical point of view, that the diffusion coefficient diverges at low temperature and scales as $T^{-\alpha}$.[48,49] The value of the parameter α was found to be 7 or 9. Nevertheless, this value depends strongly on the dimension of the system, on the strength of the interaction, and on the shape of the phonon density of states. In fact, experimental analysis in ionic insulators[50] and compound semiconductors[51] indicate that α is generally closer to 3 rather than to 7 or 9. The first observation of a T^{-7} temperature dependence was reported in a van der Waals crystal of solid nitrogen whose phonon spectrum is much closer to the Debye model.[52]

Unfortunately, there are no experimental data published for the system H/Cu(100) to compare with our calculations. However, Ho and co-workers have performed recent experiments using the scanning tunneling microscopy (STM) technique in order to determine the diffusion coefficient of hydrogen on Cu(100).[53] The authors have observed a transition between a thermally activated regime and a temperature independent regime and they report a crossover temperature close to 60 K. Moreover, it is well established that such a transition occurs for hydrogen on metals. Gomer and coworkers have shown that the system H/W (Ref. 4) and H/Ni (Ref. 8) exhibit a transition for a temperature close to 150 K and 100 K, respectively. In their experiments, the diffusion constant, below the transition temperature, appears to be strictly temperature independent. Note that, for the system H/Ni(111), the experimental situation remains unclear since Zhu and co-workers[12] found a thermally activated regime as low as 65 K and did not observe a temperature independent regime. They have observed a change in the diffusion constant around 100 K corresponding to a transition between two different thermally activated regimes. However, a theoretical analysis performed by Mattsson *et al.*[33] has confirmed the existence of a transition for this system.

In our calculations, the crossover is introduced due to phonon induced dephasing and leads to a smooth temperature dependence of the diffusion constant. In real systems, other phenomena can be responsible for the breaking of the coherent band motion such as disorder, lateral interactions, and other kinds of bosonic excitations than phonons. The disorder can arise from lattice strain or surface defects (impurities, vacancies, steps, etc.). Moreover, realistic experiments are performed at nonzero coverage and lateral interactions between adatoms have been shown to play a crucial role to reduce the mean free path of the adatom.[18] In addition, on metal surfaces, the relative influence of phonons versus electron–hole pair excitations is not clear. The electron–hole pairs in metals provide an energy dissipation mechanism in addition to the coupling to phonons. In a previous work,[17] it has been shown that the influence of these excitations can be modeled in terms of a friction coefficient. The typical value of this parameter was found to be about 1 or 3 meV. The friction coefficient can be associated to the dephasing constant. As a result, electron–hole pair excitations may play an important role in a temperature range where the dephasing constant due to phonon fluctuations is about 3 meV, i.e., $T < 50$ K.

Consequently, all these processes would have to be included in our calculations to reach the final value of the full diffusion constant. Since some of them are temperature independent, as for the inhomogeneous disorder, the final expression of the coherent part of the diffusion constant may become independent of the temperature. Moreover, the other sources of scattering contribute to the increase of the dephasing constant leading to a change of the value of the crossover temperature.

In addition, we have supposed that the quantum diffusion of the adatom could be described using a one-dimensional model. Such an approximation is valid if we assume an adiabatic decoupling between the different degrees of freedom of the adatom. Indeed, Baer *et al.*[54] have discussed the influence of the dimensionality on the thermal rate related to the transition from a subsurface hydrogen atom to a surface site of a nickel crystal. The comparison between the full three-dimensional (3D) calculations and the reduced two-dimensional (2D) and one-dimensional (1D) calculations is performed. The authors have shown that the 3D calculation exhibits the lowest thermal rate. At low temperature, the tunneling rate is nearly temperature independent and the crossover temperature was shown to decrease as the dimensionality of the calculations increases. Consequently, the authors have pointed out that the tunneling rate is very sensitive to a naive reduction of the dimensionality. Such an approximation fails, first, because of the variation of the perpendicular zero-point motion along the reaction path and second, because of the overestimation of the coherence between the two sites separated by the potential barrier. However, the authors have shown that the adiabatic approximation dramatically improves the 1D calculation. For hydrogen diffusion on the copper surface, the main contribution of the rates for incoherent hops along the x direction would involve states associated to the x motion. As a result, we thus expect a small change in the activation energy if the zero-point energies related to the y and z coordinates are the same both at the center of the site and at the top of the potential barrier along the x direction. Therefore, the incoherent diffusion constant for surface diffusion is related to the coefficient in one dimension through a symmetry factor which account for motions along equivalent high symmetry directions. However, the dephasing constant associated to a given state may become more important for a full three-dimensional problem. Indeed, the coupling with substrate phonons may induce transitions between states located in the same site but related to different coordinates. Consequently, in addition to the previous processes (disorder, lateral interactions, etc.), the dimension may affect the coherent part of the diffusion

constant and would lead to a change in the estimation of the crossover temperature.

ACKNOWLEDGMENT

This research was supported in part by Grant from the NFS-CHE9877086.

[1] *Hydrogen Effects in Catalysis*, edited by Z. Paal and P. G. Menon (Dekker, New York, 1988).
[2] G. Ehrlich and K. Stolt, Annu. Rev. Phys. Chem. **31**, 603 (1980).
[3] J. D. Doll and A. F. Voter, Annu. Rev. Phys. Chem. **38**, 413 (1987).
[4] R. DiFoggio and R. Gomer, Phys. Rev. B **25**, 3490 (1982).
[5] R. Gomer, in *Surface Mobilities on Solid Materials*, edited by V. T. Binh (Plenum, New York, 1983).
[6] C. Dharmadhickari and R. Gomer, Surf. Sci. **143**, 223 (1984).
[7] S. C. Wang and R. Gomer, J. Chem. Phys. **83**, 4193 (1985).
[8] T. S. Lin and R. Gomer, Surf. Sci. **225**, 41 (1991).
[9] S. M. George, in *Diffusion at Interfaces*, edited by M. Grunze, H-J. Kreuzer, and J. J. Weimer (Springer, Berlin, 1988).
[10] G. Binning, H. Fuchs, and E. Stoll, Surf. Sci. **169**, L295 (1986).
[11] X. D. Zhu, A. Lee, A. Wong, and U. Linke, Phys. Rev. Lett. **68**, 1862 (1992).
[12] G. X. Cao, E. Nabighian, and X. D. Zhu, Phys. Rev. Lett. **79**, 3696 (1997).
[13] K. Kitahara, H. Metiu, J. Ross, and R. Silbey, J. Chem. Phys. **65**, 2871 (1976).
[14] S. Efrima and H. Metiu, J. Chem. Phys. **69**, 2286 (1978).
[15] S. Efrima and H. Metiu, Surf. Sci. **75**, 721 (1978).
[16] G. Wahnstrom, Surf. Sci. **159**, 311 (1985); **164**, 449 (1985).
[17] G. Wahnstrom, Chem. Phys. Lett. **163**, 401 (1989).
[18] K. B. Whaley, A. Nitzan, and R. B. Gerber, J. Chem. Phys. **84**, 5181 (1986).
[19] K. F. Freed, J. Chem. Phys. **82**, 5264 (1985); A. Auerbach, K. F. Freed, and R. Gomer, *ibid.* **86**, 2356 (1987).
[20] P. D. Reilly, R. A. Harris, and K. B. Whaley, J. Chem. Phys. **95**, 8599 (1991); **97**, 6975 (1992).
[21] S. M. Valone, A. F. Voter, and J. D. Doll, Surf. Sci. **155**, 687 (1985).
[22] S. M. Valone, A. F. Voter, and J. D. Doll, J. Chem. Phys. **85**, 7480 (1986).
[23] J. G. Lauderale and D. G. Truhlar, J. Am. Chem. Soc. **107**, 4590 (1985).
[24] J. G. Lauderale and D. G. Truhlar, Surf. Sci. **164**, 558 (1985).
[25] G. Wahnstrom, J. Chem. Phys. **89**, 6996 (1988).
[26] J. G. Lauderale and D. G. Truhlar, J. Chem. Phys. **84**, 1843 (1986).
[27] T. N. Truong and D. G. Truhlar, J. Chem. Phys. **88**, 6611 (1988).
[28] S. E. Wonchoba and D. G. Truhlar, J. Chem. Phys. **99**, 9637 (1993).
[29] Y. Sun and G. A. Voth, J. Chem. Phys. **98**, 7451 (1993).
[30] K. Haug, G. Wahnstrom, and H. Metiu, J. Chem. Phys. **92**, 2083 (1990).
[31] D. H. Zhang, J. C. Light, and S. Y. Lee, J. Chem. Phys. **111**, 5741 (1999).
[32] T. R. Mattsson, G. Wahnstrom, L. Bengtsson, and B. Hammer, Phys. Rev. B **56**, 2258 (1997).
[33] T. R. Mattsson and G. Wahnstrom, Phys. Rev. B **56**, 14944 (1997).
[34] J. Rammer, *Quantum Transport Theory* (Perseus Books, Massachusetts, 1998).
[35] J. Rammer, Rev. Mod. Phys. **63**, 781 (1991).
[36] E. Wigner, Phys. Rev. **40**, 749 (1932).
[37] L. E. Reichl, in *A Modern Course in Statistical Physics*, edited by E. Arnold (1980).
[38] R. Zwanzig, Lect. Theor. Phys. **3**, 106 (1960).
[39] G. P. Srivastava, *The Physics of Phonons* (Adam Hilger, New York, 1990).
[40] P. Resibois, J. Stat. Phys. **2**, 21 (1970).
[41] J. C. Light, R. M. Whitnell, T. J. Park, and S. E. Choi, ''Supercomputer algorithms for reactivity,'' in *Supercomputer Algorithms for Reactivity, Dynamics and Kinetics of Small Molecules* (Kluwer Academics, Boston, 1989), p. 187.
[42] M. S. Child, *Semiclassical Mechanics with Molecular Applications* (Clarendon, Oxford, 1991).
[43] K. P. Bohnen, T. Rodach, and K. M. Ho, in *Surcture of Surfaces-III*, edited by S. Y. Tong, M. A. Van Hove, X. Xie, and K. Takayanagi (Springer, Berlin, 1991).
[44] Y. Chen, S. Y. Tong, J-S. Kim, L. L. Kesmodel, T. Rodach, K. P. Bohnen, and K. M. Ho, Phys. Rev. B **44**, 11394 (1991).
[45] W. Kress and F. W. de Wette, *Surface Phonons* (Springer, Berlin, 1991).
[46] P. Zeppenfeld *et al.* Phys. Rev. B **38**, 12329 (1988).
[47] V. G. Storcak and N. V. Prokof'ev, Rev. Mod. Phys. **70**, 929 (1998).
[48] A. F. Andreev and I. M. Lifshitz, Sov. Phys. JETP **29**, 1107 (1969).
[49] Yu. Kagan and L. A. Maksimov, Sov. Phys. JETP **38**, 307 (1974).
[50] R. F. Kiefl, R. Kadono, J. H. Brewer, G. M. Luke, H. K. Yen, M. Celio, and E. J. Ansaldo, Phys. Rev. Lett. **62**, 792 (1988).
[51] R. Kadono, R. F. Kiefl, E. J. Ansaldo, J. H. Brewer, M. Celio, S. R. Kreitzman, and G. M. Luke, Phys. Rev. Lett. **64**, 665 (1990).
[52] V. G. Storcak, J. H. Bewer, and G. D. Morris, Phys. Lett. A **193**, 199 (1994).
[53] L. J. Lauhon and W. Ho (unpublished).
[54] R. Baer, Y. Zeiri, and R. Kosloff, Phys. Rev. B **58**, R5287 (1996).